Incorrect Folding of Steroidogenic Acute Regulatory Protein (StAR) in Congenital Lipoid Adrenal Hyperplasia†

Himangshu S. Bose,‡ Michael A. Baldwin,§,|| and Walter L. Miller*,‡,⊥

Departments of Pediatrics, Neurology and Pharmaceutical Chemistry, and The Metabolic Research Unit, University of California, San Francisco, San Francisco, California 94143-0978

Received March 16, 1998; Revised Manuscript Received May 15, 1998

ABSTRACT: Steroidogenic acute regulatory protein (StAR) rapidly stimulates the movement of cholesterol into adrenal and gonadal mitochondria to mediate the acute steroidogenic response; StAR mutations cause potentially lethal congenital lipoid adrenal hyperplasia (lipoid CAH). Bacterially expressed wild-type StAR and four amino acid replacement/deletion mutants that cause lipoid CAH were purified to apparent homogeneity. Sedimentation equilibrium ultracentrifugation showed that all five proteins were monomeric and fit a globular protein model of the correct molecular mass. Circular dichroism (CD) spectra of both the wild-type and mutants showed minima near 208 and 222 nm, confirming the presence of substantial α-helical structure. However, subtle differences in the CD signals of the wild-type and mutants in the far-UV and stronger differences in near-UV indicated differences in protein folding. The amide I and II bands in the 1400−1700 cm^{-1} region of Fourier transform infrared spectra showed that the proteins fell into two groups. The wild-type and a partially active conservative mutant were predominantly α-helical with some intramolecular β-sheet. By contrast, three mutants that lost charged residues retained much of their α-helical structure, but also tended to form intermolecular β-sheets. Urea at 2.0 or 4.0 M had less effect on the CD spectrum of the wild-type than of the mutants, particularly those having lost a charged residue; 50 mM guanidinium hydrochloride did not alter the CD spectrum of the wild-type, but elicited dramatic changes to the secondary structure in all four mutants. Despite this, thermal melting curves of the mutant proteins in 50 mM guanidinium hydrochloride showed surprising stability, even exceeding that of the wild-type protein. These data suggest that the StAR amino acid replacement mutants that cause lipoid CAH are inactive because of fairly gross errors in protein folding, probably due to the loss of salt bridges that stabilize the tertiary structure.

The first step in the biosynthesis of all steroid hormones, including glucocorticoids, mineralocorticoids and sex steroids, is the conversion of cholesterol to pregnenolone by the cholesterol side-chain-cleavage enzyme, P450scc, which resides on the inner mitochondrial membrane (*1*). The adrenal cortex and gonads exhibit both acute regulation of steroidogenesis, which occurs within minutes, and chronic regulation, which occurs over hours and days, whereas steroidogenesis in the placenta and brain appears to exhibit only chronic regulation (*2*−*5*). The acute response is mediated by providing increased cholesterol substrate to P450scc (*2*−*5*), while the chronic response is largely mediated by increased transcription of the genes for P450scc and the other steroidogenic enzymes (*6*). The steroidogenic acute regulatory protein (StAR),[1] a 30 kDa phosphoprotein that is synthesized rapidly in response to cAMP and which has a very short half-life (*7*, *8*), has been cloned and characterized from rat (*9*) and human (*4*) sources. Transfection of steroidogenic (*9*) and nonsteroidogenic (*3*, *4*) cells shows that StAR increases steroidogenesis at least 6-fold. Disruption of the human StAR gene causes lipoid CAH (*3*, *5*, *10*, *11*), a severe disorder of adrenal and gonadal steroidogenesis (*12*) in which placental steroidogenesis is spared (*13*), (for review, see ref *14*).

StAR is synthesized as a 285 amino acid protein imported into mitochondria via a typical mitochondrial leader sequence (*2*, *9*, *15*). However deletion of up to 62 amino-terminal amino acids including the entire leader results in a cytoplasmic protein that retains at least 100% of its activity and appears to interact with the outer mitochondrial membrane (*16*). Furthermore, deletion of only 10 carboxy-terminal amino acids destroys StAR activity (*16*), and all amino acid replacement mutations that have been shown to cause lipoid

† This work was supported by NIH Grants DK37922, DK42154, and HD34449, and by a grant from the March of Dimes, all to W.L.M. Mass spectrometry was carried out in the UCSF Mass Spectrometry Facility (Director, A. L. Burlingame), supported by NIH NCRRBRTP RR01614.

* Author to whom all correspondence should be addressed at Dept. of Pediatrics, Bldg. MR-IV, Box 0978, University of California, San Francisco, San Francisco, CA 94143-0978.

‡ Dept. of Pediatrics.

§ Dept. of Neurology.

|| Dept. of Pharmaceutical Chemistry.

⊥ The Metabolic Research Unit.

[1] Abbreviations: CD, circular dichroism; FTIR, Fourier transform infrared spectroscopy; GnHCl, guanidinium hydrochloride; HPLC high-performance liquid chromatography; IPTG, isopropyl β-D-thiogalactopyranoside; lipoid CAH, congenital lipoid adrenal hyperplasia; N-62, StAR proteins lacking 62 amino-terminal amino acids; PCR, polymerase chain reaction; PMSF, polymethylene sulfonyl fluoride; PVDF, polyvinylidine difluoride; SDS, sodium dodecyl sulfate; StAR, steroidogenic acute regulatory protein; TFA, trifluoroacetic acid; UV, ultraviolet.

S0006-2960(98)00588-1 CCC: $15.00
Published on Web 06/18/1998

CAH lie in the carboxy-terminal 40% of the StAR sequence (*5*, *11*). Thus it appears that the carboxy-terminal half of the protein is crucial for interaction with an as-yet unidentified protein on the outer mitochondrial membrane, possibly the peripheral benzodiazapine receptor (*17*). To begin to understand how the StAR protein is folded and how these amino acid replacements disrupt its function, we have performed physical and spectroscopic analysis of the wild-type and four naturally occurring replacement mutants that cause lipoid CAH.

MATERIALS AND METHODS

Construction of StAR Expression Plasmids. The wild-type and mutant StAR proteins were expressed as the active forms lacking the 62 amino-terminal amino acid residues (N-62) (*16*). The wild-type N-62 StAR sequence was constructed by amplification of the cloned human cDNA using the primers 5′ATCGGATCCGATGACGATGACAAAATG-GAAGAGACTCTCTAC3′ (E3S) and 5′AGCTAAGCTTTG-GTCTTCAACACCTGGCT3′ (EAS) and PCR program # 4 (*18*). The N-62 StAR sequences for the mutants E169G, R182L, ΔR272, and L275P were prepared by PCR amplification of our previously constructed eukaryotic vectors for these mutants (*5*) using the same E3S/EAS primer combination. To build the N-62 L275P construct, an initial PCR was done with E3S and 5′ACCTGGCTTCAGAGGC-AGGGTGGGACTCCGGGCGCTTGCGC3′ as the antisense primer using program #4, followed by a second PCR amplification with primers E3 and EAS. The underlined nucleotides are identical with EAS, and the underlined italicized G is the mutated nucleotide. The various PCR-amplified DNAs were digested with *Bam*HI and *Hin*dIII, electrophoresed through 1.2% agarose gel, purified through Qiagen columns, ligated into pQE30 predigested with *Bam*HI and *Hin*dIII, and cloned into *Escherichia coli* DH5α. The accuracy of the constructs was confirmed by sequencing both strands of each clone. Constructs were then transformed into competent *E. coli* M15 (pREP4), grown in LB medium containing 30 μg/mL kanamycin and 100 μg/mL ampicillin to OD = 0.6, and induced with 1 mM isopropyl β−D-thiogalactopyranoside (IPTG) (Figure 1A). The bacteria were pelleted by centrifugation and resuspended in 3 mL/g *E. coli* lysis buffer (*19*) containing 1 mM polymethylene sulfonyl fluoride (PMSF).

Expression of Soluble Bacterial StAR Protein. E. coli cultures were grown in SOC medium (*19*) containing 50 mM glucose at 37 °C with shaking at 100 rpm. At OD = 0.3, the culture was transferred to a 20−22 °C incubator shaking at 30 rpm and induced overnight with 0.4 mM IPTG. The bacteria were harvested at 37000*g*, washed twice with 1 mM $MgCl_2$, 10 mM Tris-HCl, pH 8.0, and stored at −70 °C overnight. Frozen bacterial pellets were thawed at room temperature for 30 min, then 5 mL of 10 mM Tris-HCl, pH 8.0, 100 mM NaH_2PO_4, 8.0 M urea, 10 mM imidazole (buffer A) and 10 μL each DNase I and RNase I (10 mg/mL) were added per gram of bacterial pellet and incubated on ice. After 30 min, the bacterial lysate was no longer viscous and was spun at 37000*g* for 30 min at 4 °C. The supernatant was stored, and the bacterial pellet was reprocessed as described for the original bacterial pellet. The supernatant was loaded onto a 20 mL bed volume Ni-NTA super flow column (Qiagen) precharged with $NiSO_4$ and equilibrated with buffer A. The column was washed with 10 bed volumes of buffer A and 10 bed volumes of 10 mM Tris-HCl, pH 6.3, 100 mM NaH_2PO_4, 40 mM imidazole, 8.0 M urea, and 500 mM NaCl. The column was rewashed with 5 bed volumes of buffer A, modified to pH 5.8. Finally the Ni^{2+}−His bond was broken, and the StAR protein eluted with 300 mM imidazole containing 10 mM Tris-HCl, pH 4.5, 100 mM NaH_2PO_4, and 8.0 M urea. The purity of the protein was monitored by electrophoresis on 12.5% SDS−polyacrylamide (Figure 1B). The eluted protein was dialyzed against 8.0 M urea, 10 mM Tris-HCl buffer, pH 8.3, through a 12−14 kDa cutoff membrane for 48 h at room temperature, and then against 6.0 M urea, 10 mM Tris-HCl, pH 8.3, while the temperature was gradually dropped to 4 °C over 24 h. The urea concentration was then gradually decreased to zero in 0.2 M intervals every 6 h. The protein was finally dialyzed against 10 mM Tris-HCl, pH 8.3, for 2−3 days, changing the dialysis buffer every 12 h.

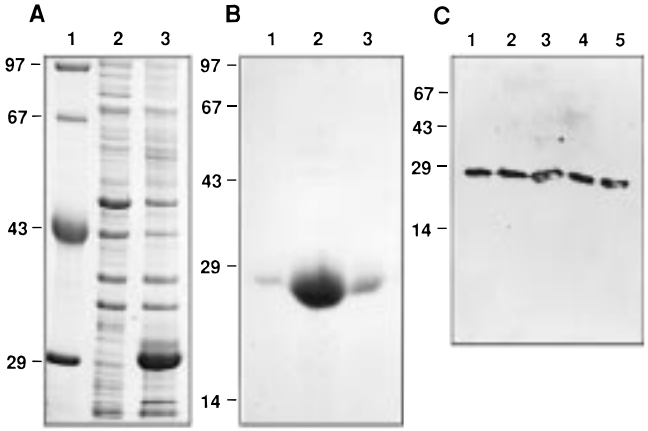

FIGURE 1: Bacterial expression of StAR. Panel A: SDS−polyacrylamide gel. Lane 1, molecular weight markers; lane 2, uninduced; lane 3, induced with IPTG. Panel B: SDS−polyacrylamide gel of material eluted from the Ni-NTA column. Lane 1, before elution; lane 2, after elution with 15 mL 300 mM imidazole; lane 3, further elution with 15 mL 300 mM imidazole. Approximately 100 μg was loaded per lane. Panel C: Western Blot. Recombinant StAR protein and mutants were subjected to 12.5% SDS−PAGE, and western blotted as described (*3*). Lane 1, wild-type; lane 2, E169G; lane 3, R182L; lane 4, ΔR272; lane 5, L275P. In panels B and C, molecular weight markers were run in other lanes not shown.

Western Blotting. The affinity-purified recombinant N-62 StAR protein (100 ng) was electrophoresed through 12.5% SDS polyacrylamide gel, electroblotted to polyvinylidine difluoride (PVDF) membrane (Millipore), and immunostained with a polyclonal rabbit anti-human StAR antiserum (a gift from Prof. Douglas Stocco). The membrane was blocked with 5% nonfat dry milk for 45 min followed by overnight probing with the antibodies and incubation with peroxide-conjugated with goat anti-rabbit IgG (Sigma), then developed with ECL reagent (Amersham).

Chromatography and Mass Spectrometry. An aliquot of the dialyzed recombinant StAR protein was separated by reverse-phase HPLC with a C-4 Vydac column using 0.06% trifluoroacetic acid (TFA) as solvent A and 0.052% TFA in 80% acetonitrile as solvent B, with UV absorbance at 214 nm. Fractions were collected across the peak and analyzed by electrospray mass spectrometry (Perseptive Biosystems Mariner). A further aliquot of the dialyzed protein was separated by anion exchange chromatography using a Phar-

macia Mono-Q column and was eluted with 1.0 M NaCl with UV absorbance monitored at 279 nm.

Analytical Ultracentrifugation. Sedimentation equilibrium analyses of wild-type and mutant StAR in 10 mM Tris-HCl, pH 8.3, were performed with a Beckman XLA ultracentrifuge equipped with absorption optics, at 10000 rpm at 20 °C for 40 h. The concentration of the wild-type protein was ~0.3 mg/mL, giving an absorbance of 0.326 at 279 nm. The molecular mass was calculated from the sedimentation equilibrium runs using a computer program that adjusts the baseline absorbance to obtain the best linear fit of ln A versus r^2, where A is the absorbance, and r is the distance from the radius to the cell. This program calculates a molecular mass from the experimental data based on a model globular protein.

UV Spectroscopy. Ultraviolet (UV) absorption spectra of protein samples (300 μg/mL) were measured in a Shimadzu 160U spectrophotometer in a masked quartz cuvette of 1 mm path length. The buffer baselines and sample spectra were recorded at room temperature after constant time intervals of 2, 6, 12, 24, and 48 h.

CD Spectroscopy. Far-UV (195−250 nm) circular dichroism (CD) measurements were carried out in a 1.0 mm path length cuvette at 300 μg protein/mL (1.52×10^{-6} M) in 10 mM Tris-HCl, pH 8.3, at 20 °C in a Jasco J-720 spectropolarimeter. Protein concentrations were determined spectrophotometerically after guanidinium hydrochloride (GnHCl) denaturation (*20*) for all spectroscopic studies. Near-UV (250−360 nm) measurements were made using a 1.0 cm quartz cuvette at 3 mg protein/mL; multiple scans were averaged to improve the signal-to-noise ratio. Appropriate buffer baselines were obtained under the same experimental conditions and were subtracted from the sample spectra; data are shown as mean residue ellipticity $[\theta]_r$. In some spectra the noise was reduced by application of a Savitsky−Golay filter.

Fourier Transform Infrared Spectroscopy (FTIR). Samples for FTIR were dissolved in D_2O (Aldrich), equilibrated for 48 h, dried as a thin film on a calcium fluoride window, and analyzed over the frequency range 2000−1000 cm^{-1} in an infrared microscope attached to a Perkin-Elmer system 2000 FTIR spectrophotometer at 2 cm^{-1} resolution. The microscope housing was flushed with dry nitrogen, and 100 background spectra were accumulated; sample spectra were then recorded under the same conditions until any water vapor signal was canceled out. Least-squares interactive Gaussian curve fitting was carried out to the amide I band in the region 1700−1600 or 1700−1550 cm^{-1}, corrected for the spectrum of buffer alone recorded under identical conditions.

Melting Studies and Denaturants. Thermal denaturation curves were obtained by measuring the CD signal at 222 nm as a function of temperature from 5° to 80 °C. The temperature was increased 2 °C per minute with a step resolution 0.5 °C. The reversibility of thermal unfolding was checked to the initial value at 5 °C. The effects of denaturants were determined using urea and GnHCl. Thermal unfolding was compared in pH 8.3 sodium phosphate buffer with and without 50 mM GnHCl.

Preparative Ultracentrifugation. StAR proteins at concentrations between 0.65 and 1.0 mg/mL (A_{280} between 0.48 and 0.88) were centrifuged at 100000*g* for 1 h at 20 °C in a Beckman TLA 100.3 rotor in a TL-100 centrifuge in either 10 mM Tris-HCl, pH 8.3, or in 50 mM GnHCl, 10 mM Tris-HCl, pH 8.3, and the absorption at 280 nm was measured before and after to assess the portion remaining in the solution.

RESULTS

Expression and Purification of Recombinant StAR. To produce biochemically useful quantities of StAR protein, the 223 amino acid N-62 structure, which retains full biological activity (*16*), was placed under the control of the inducible T5 promoter and *lac* operator sequences and expressed in *E. coli*. A start codon was placed at the amino terminus followed by six histidine codons (His_6) and an enterokinase protease recognition site (Asp_4−Ala), facilitating the purification of the expressed fusion protein on metal affinity resins. The *E. coli* host contained multiple copies of plasmid pREP4, which carries the *lac*I gene encoding *lac* repression. Induction with IPTG led to rapid inactivation of the repressor and activation of the promoter allowing the expression of a predominant polypeptide (Figure 1A). Digestion was completed by overnight incubation at 21 °C with 1 U of enterokinase (Novagen) per 25 mg of protein.

Induction with IPTG resulted in robust expression of StAR protein. No other protein species were seen when 100 μg of purified protein was displayed by gel electrophoresis (Figure 1B). The calculated molecular mass of the final N-62 wild-type StAR protein, including the linker, is 26 934 Da. Both the wild-type and mutants had similar apparent molecular weights and reactivity with antisera directed against human StAR (Figure 1C). The purity of the StAR protein was confirmed by anion exchange chromatography (not shown), giving a single peak eluting in 1.0 M NaCl, irrespective of the presence or absence of urea, consistent with the acidic nature of this protein (*7*, *8*) and the calculated isoelectric point (pI) of 5.82. It was also separated by reverse-phase HPLC, from which the protein eluted at ~40% solvent B. Fractions were collected across the peak and analyzed by electrospray mass spectrometry. Early fractions revealed addition of multiple oxygen atoms, probably due to aerobic formation of methionine sulfoxide during the purification; later fractions were close to the calculated mass, although the protein could not be purified completely devoid of any oxygen.

Analytical ultracentrifugation showed that the wild-type and mutant StAR proteins were monomeric without significant dimerization or aggregation. The analytical data for each protein were in excellent agreement with the globular protein model, as shown by the random distribution of residuals between the experiment and calculated functions. The data for the E169G mutant (Figure 2) were typical of all five proteins. The molecular masses of the N-62 proteins derived from the centrifugation data compared favorably with the calculated values (Table 1).

CD Spectroscopy. As the purification procedure for large quantities of bacterially produced StAR required denaturation and refolding, we first sought to determine if the refolding procedure yielded the native conformation. As no in vitro assay for StAR activity is available, we prepared native StAR by growing bacteria at 15 °C and preparing soluble cytosolic StAR by nickel column chromatography without denaturation

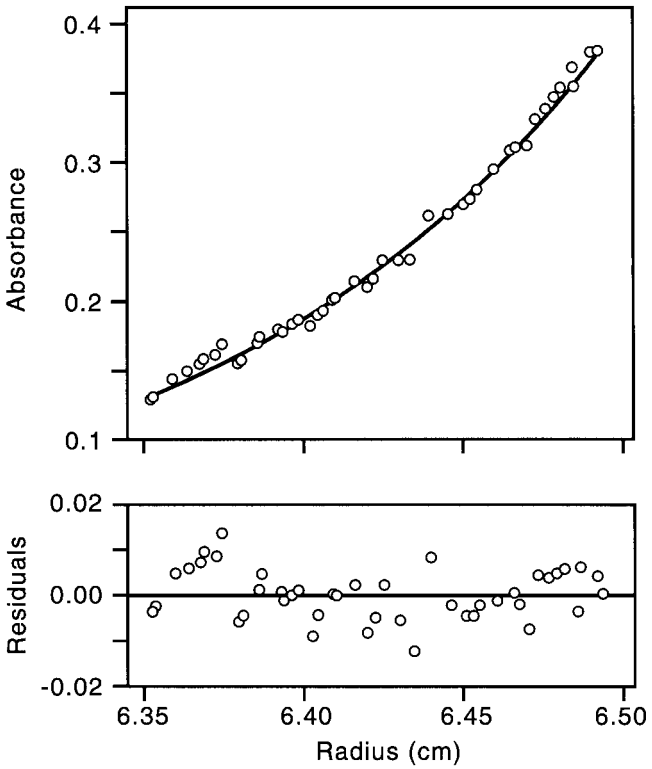

FIGURE 2: Sedimentation equilibrium. Wild-type and mutant StAR proteins were spun at 10000 rpm in 10 mM Tris-HCl, pH 8.3, at 20 °C, and the absorbance at 279 nm was recorded. The proteins attained equilibrium after 24 h, and the experiment was continued to 40 h. The profiles of all five proteins looked essentially the same; the profile shown is for the E169G mutant. (Above) sedimentation profile, (below) residuals (distribution of deviations from theoretical).

Table 1: Molecular Weights of N-62 StAR Proteins

N-62 StAR Protein	calculated MW	observed[a]
wild-type	26 934	26 413
E169G	26 862	26 887
R182L	26 891	27 251
ΔR272	26 778	27 328
L275P	26 918	27 421

[a] Computer-generated value from sedimentation equilibrium.

in urea. Only a small amount of protein could be obtained in this fashion, but its CD spectrum was indistinguishable from the denatured/refolded StAR (Figure 3A). Thus the refolding procedure yields the native conformation.

The CD spectrum of the wild-type StAR protein at pH 8.3 in 10 mM sodium phosphate buffer or 10 mM Tris-HCl gave minima in the vicinity of 222 and 208 nm, indicating α-helical structure. Under nondenaturing conditions the wild-type and all four mutants gave similar spectra at the $\pi-\pi^*$ (208 nm) and $n-\pi^*$ (222 nm) transitions, respectively, with only subtle differences in wavelength and ellipticity (Figure 3B). The patterns were characteristic of α-helix. Techniques for determining secondary structure from CD curves have been reviewed recently (*21*); a theoretical prediction using the PHD method (*22*) suggested that the protein is about 38% α-helix, 21% β-sheet, and 41% loops. This is consistent with the strength of the molar ellipticity at 208 nm, which suggests the presence of substantial α-helical structure (*23*). Similarly, analysis of the experimental data with two widely used computational algorithms (*24*, *25*) gave values of about 35% α-helix.

The far-UV CD spectra of most proteins with large amounts of α-helix are generally insensitive to changes in secondary structural elements other than α-helix, and they rarely reveal differences in the tertiary structure. Thus, although the CD data in Figure 3B suggest that both the wild-type and mutant StAR proteins are predominantly α-helical, they could be folded differently, and the spectra do not exclude the possibility that the mutants might differ from one another in their tertiary folding. This would apply particularly if mutations could disrupt interactions between secondary structural elements by interfering with hydrophobic interactions, salt bridges, or disulfide bonds (*26*−*28*).

To investigate further the differences in folding between the wild-type and mutant StAR proteins, we monitored near-UV CD spectroscopy in the range 250−360 nm (Figure 3C). Positive or negative features in this region of a CD spectrum are most often associated with orientation and environment of the aromatic amino acid side chains between secondary structures, and they confirm that a protein is folded (*29*). The wild-type StAR and its mutants all possessed tertiary structure, but there were differences, particularly in the region 259−291 nm (Figure 3C). The greatest differences were seen with the E169G and ΔR272 mutants, showing that the loss of certain charged amino acids had the greatest effects on tertiary structure. Somewhat surprisingly, the R182L mutant showed no corresponding differences in its near-UV spectrum, although this does not rule out a structural change.

Proteins that contain amphipathic α-helices may aggregate cooperatively in aqueous solution. In such aggregates the hydrophobic domains of amphiphilic helices generally interact to form a hydrophobic core (*30*). To evaluate whether such a self-association process might occur with the StAR protein, we analyzed the CD spectra following overnight freezing at −20 °C and thawing for 16 h at room temperature. The frozen and thawed protein had the same ellipticity as StAR protein that had not been frozen (not shown), with approximately equal proportions of α-helical conformation, suggesting that the thawed protein refolded to its original conformation.

Fourier Transform Infrared Spectroscopy. CD spectra tend to be dominated by α-helical structure, and FTIR spectra may fail to distinguish between α-helices and random coils, but FTIR spectra are very sensitive to the presence of β-sheets and can generally distinguish between intramolecular and intermolecular β-sheets. Thus FTIR and CD data are highly complementary. FTIR can be done with great sensitivity on thin films, yielding spectra that differ little from the corresponding spectra obtained in solution (*31*). FTIR spectra generally display two major bands in the region 1700−1400 cm^{-1} associated with the so-called amide I and amide II vibrations (Figure 4A). The amide I band, which usually occurs at 1700−1600 cm^{-1} is the strongest indicator of secondary structure (*32*), with random coil at ∼1637−1645 cm^{-1}, α-helix at ∼1645−1662 cm^{-1}, and β-turns at ∼1663−1680 cm^{-1} (*33*−*35*). β-Sheet vibrations are split into strong low-frequency (<1637 cm^{-1}) and weaker high-frequency (>1680 cm^{-1}) bands; intermolecular β-sheets display the greatest degree of splitting and are frequently observed at <1620 cm^{-1} (*32*).

The FTIR spectra obtained for thin films of wild-type and mutant StAR proteins over the frequency range 2,000−1,-

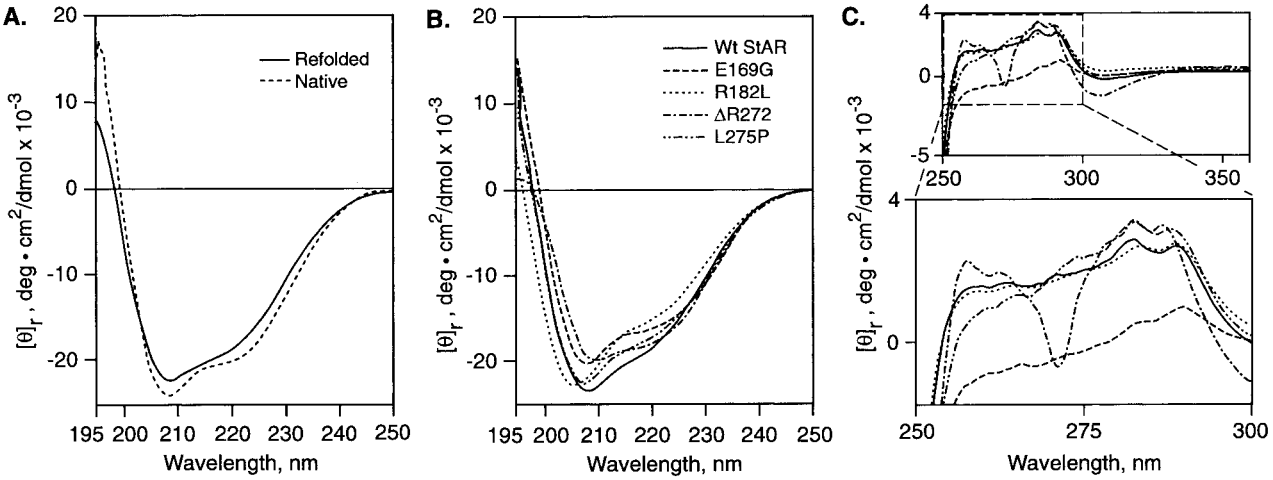

FIGURE 3: CD spectra of StAR proteins at pH 8.3, at 20 °C. The spectrum of the buffer blank was subtracted from the experimental samples. The data shown are the average of 20 scans with a step resolution 0.5 nm. Panel A: Far-UV CD spectrum at 195−250 nm of native and refolded wild-type StAR proteins at pH 8.3 and a concentration of 0.3 mg/mL. Panel B: Far-UV CD spectrum of StAR proteins at pH 8.3 and a concentration of 0.3 mg/mL. Panel C: (Top) Near-UV CD spectrum at 250−360 nm of StAR proteins and a concentration of 3.0 mg/mL. (Below) Enlarged view of near-UV spectrum from 250 to 300 nm. In all panels: wild-type StAR (—), E169G (- - -), R182L (···), ΔR272 (- · - · -), L275P (- ·· - ·· -).

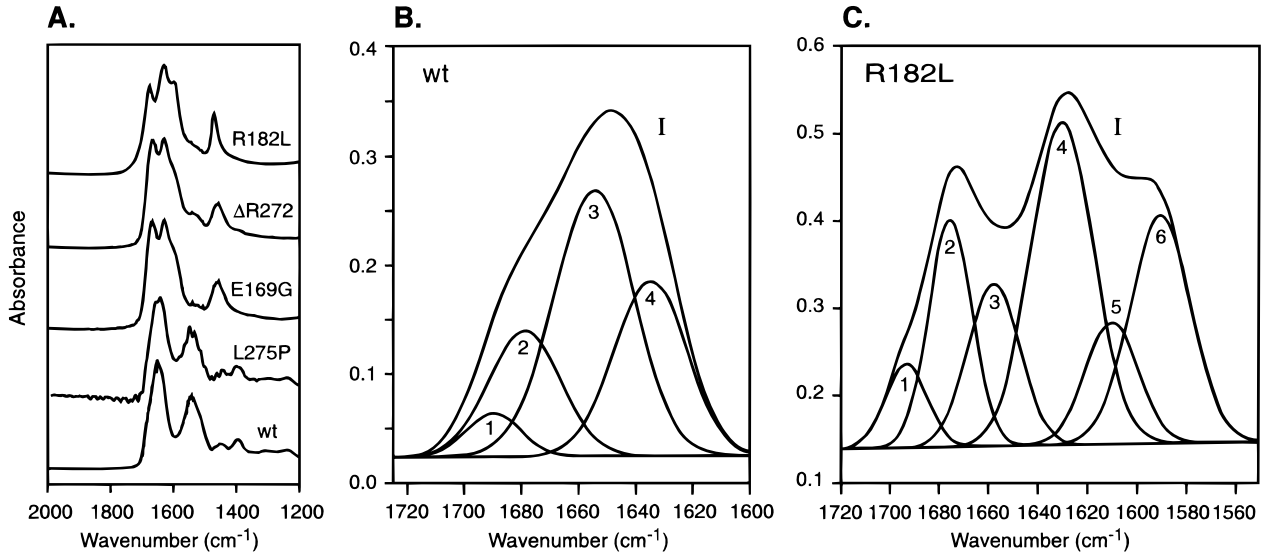

FIGURE 4: Fourier transform infrared spectra of the wild-type and mutant StAR proteins equilibrated with D_2O for 48 h in 10 mM Tris-HCl, pH 8.3. Panel A: Spectra of all five proteins (the absorbance scale is in arbitary units). The amide I peak reaches a maximum at 1649 cm^{-1}, and the amide II peak reaches its maximum at 1544 cm^{-1}. Panels B and C: Curve fitting to the amide I peak after subtraction of the spectrum of the buffer for the wild-type (Panel B) and R182L (Panel C) StAR proteins. The noise in the amide I peak was reduced by a Savitsky−Golay filter and is shown as the topmost line. The second derivative can be resolved into various component peaks labeled 1−4 (wild-type) or 1−6 (R182L).

000 cm^{-1} (Figure 4A) could be divided into two distinct groups. The wild-type and L275P mutant exhibited almost identical spectra, having conventional amide I and II bands with the amide I band centered at ∼1650 cm^{-1}, consistent with the proteins possessing a large degree of α-helical structure. By contrast, the E169G, R182L, and ΔR272 mutants gave similar but unusual spectra in which the amide II band was weakened and the amide I was shifted to lower wavenumbers (i.e., lower vibrational frequencies), particularly for R182L.

The secondary structure was probed further by comparing peak-fitting analysis of the amide I profiles for the wild-type and all four mutants; the wild-type (Figure 4B) and R182L mutant (Figure 4C) are shown as representative of each group. Peak-fitting algorithms rarely give unique solutions as numerous variables are at the discretion of the operator; i.e., the number of peaks, possible limits to their widths, frequencies and heights, and the choice of Lorentzian versus Gaussian line shapes. Nevertheless judicious use of this method can provide clues to the likely secondary structure content (*35*). Analysis of the wild-type spectrum confirmed the presence of a major band due to α-helix at 1658 cm^{-1}; other components at 1680 and 1690 cm^{-1} could represent β-turns and/or a high-frequency β-sheet vibration respectively; a substantial component at 1637 cm^{-1} was almost certainly attributable to intramolecular β-sheet. Thus the FTIR spectrum was wholly consistent with the CD data for the wild-type protein and suggested that the relatively conservative hydrophobic mutation L275P did not alter the StAR structure dramatically.

By contrast, deconvolution and peak fitting to the charge mutants (R169G, R182L, and ΔR272) demonstrated some

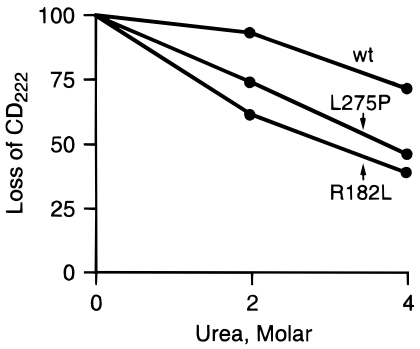

FIGURE 5: Effect of urea on far-UV CD spectrum. The CD spectra of the wild-type and the R182L and L275P mutants were recorded between 210 and 250 nm in the presence of 0.0, 2.0, and 4.0 M urea. The ellipticity of each protein at 222 nM in 0.0 M urea was arbitrarily set at 100% and is compared to the corresponding CD_{222} in 2.0 and 4.0 M urea. Urea exerts a modest destabilizing effect on the wild-type and a progressively greater effect on the L275P and R182L proteins.

unusual features, particularly for R182L, which showed the greatest differences from the wild-type spectrum (Figure 4C). The CD spectra for all of the mutants had implied that all retained a significant amount of α-helix, consistent with the observation for R182L of an FTIR peak at 1658 cm^{-1}, although this was less intense than the corresponding peak in the wild-type spectrum. The β-turns and high-frequency β-sheets could also be identified as peaks at 1676 and 1694 cm^{-1}, respectively. The most striking difference in the FTIR spectrum of the R182L mutant compared with the wild-type and L272P mutant was the increase in β-sheet at 1630 cm^{-1} and the substantial shift of a portion of this to less than 1600 cm^{-1}. Although analytical centrifugation showed that all five proteins were monomeric in solution, it is likely that the mutants that showed the low-frequency β-sheet were interacting in the thin films and forming intermolecular sheets. Thus the choice of thin films for FTIR highlighted dramatic differences in the behavior of the mutants which would not have been seen with FTIR of the proteins in solution. As this behavior was manifest only for the mutants that had lost charged residues, we conclude that the mutations had destroyed stabilizing salt bridges and the proteins had undergone different tertiary folding.

Thermal Melting and the Effects of Urea and Guanidine Hydrochloride. Wild-type and mutant StAR proteins in sodium phosphate buffer all displayed a high degree of resistance to heat denaturation up to 85 °C, as monitored by the loss of CD signal at 222 nm (data not shown). Thus the StAR secondary structure is unusually stable to heat.

Modest concentrations of denaturants such as urea or guanidine generally unfold protein tertiary structure before unfolding secondary structure, and they maintain the protein in a soluble form without aggregation, presumably by binding directly to the protein (*36*, *37*). At higher concentrations the secondary structure is likely to be lost. The wild-type protein lost some CD signal at 222 nm in 2.0 and 4.0 M urea, but the effect was greater for the hydrophobic mutant L275P and even greater for the charged-residue mutant R182L (Figure 5). Thus the wild-type protein appeared to be significantly more stable than the mutants; furthermore, although many proteins would be denatured by 4.0 M urea to give a random coil, both the wild-type and the mutants are significantly resistant to denaturation by urea.

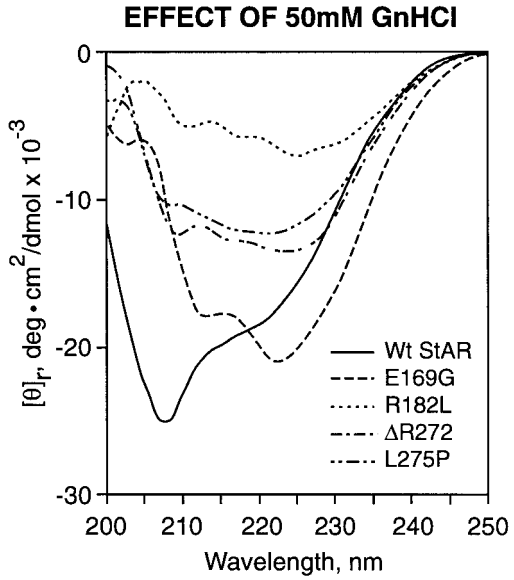

FIGURE 6: Far-UV CD spectrum of StAR proteins in the presence of 50 mM guanidinium hydrochloride at pH 8.3 and a protein concentration 0.3 mg/mL at 20 °C. Multiple scans between 200 and 250 nm with a step resolution 0.5 nm/min were averaged. Wild-type StAR (—), E169G (- - -), R182L (···), ΔR272 (- · - · -), L275P (- ·· - ·· -).

Guanidine is usually a more powerful denaturant than urea, partly because urea is an uncharged molecule that has less effect on intermolecular electrostatic interactions than guanidine, which is cationic. GnHCl at the very low concentration of 50 mM had no effect on the CD spectrum of wild-type StAR, but it dramatically changed the spectra of the mutants (Figure 6). The effect of GnHCl on the StAR mutants is specific and is not due to ionic strength; NaCl concentrations up to 0.5 M had no significant effects on the far-UV CD spectra of either the wild-type or any of the four mutant StAR proteins (results not shown). None of the modified spectra in GnHCl were amenable to a simple interpretation, but they all showed a loss of signal in the region between 210 and 225 nm. Such an observation would generally imply a loss of secondary structure, but there was no correspondingly increased negative signal at lower wavelengths, which would be anticipated for a concomitant formation of random coil. Thus it appeared that GnHCl caused partial aggregation of the mutant proteins. That this should occur with the mutants but not the wild-type StAR would be consistent with our suggestion that they are substantially different in their tertiary structure.

Additional evidence for aggregation was seen in the melting curves obtained in the presence of 50 mM GnHCl. Although the StAR mutants were resistant to melting in the absence of GnHCl, their secondary structure was somewhat destabilized in its presence and all five proteins had remarkably similar melting profiles (Figure 7). The curves for some of the mutants such as E169G were broadened, implying that the disaggregation occurred over a wide temperature range; others such as L275P were parallel with the wild-type, suggesting cooperativity between disaggregation and unfolding. It should be noted that these are not classical melting curves as, with the exception of the wild-type, the structures represented by the CD signal at 222 nm are not known, thus the choice of this wavelength was arbitrary.

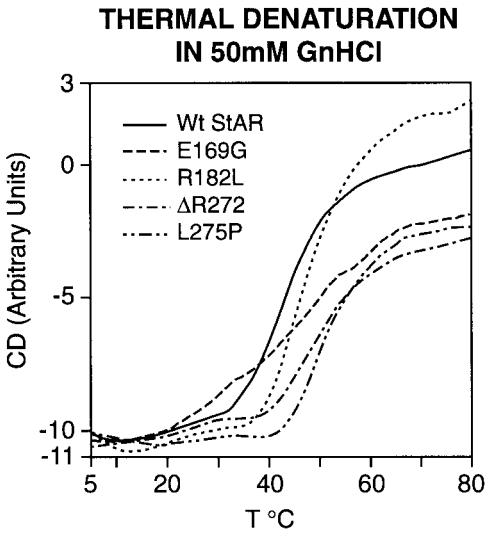

FIGURE 7: Thermal denaturation. Denaturation of StAR protein in the presence of 50 mM guanidinum hydrochloride in 10 mM sodium phosphate, pH 8.3, recorded by CD at 222 nm. GnHCl was added to the protein solution and equilibrated overnight, then the temperature was increased from 5 to 80 °C. Wild-type StAR (—), E169G (- - -), R182L (•••), ΔR272 (- • - • -), L275P (- •• - •• -).

As the wild-type and mutants were monomeric on analytical ultracentrifugation in 10 mM Tris-HCl (Figure 2), we found it most remarkable that a low, 50 mM concentration of GnHCl should provide spectroscopic evidence of selective aggregation of all four mutants but not the wild-type. Therefore, to test the aggregation hypothesis directly we subjected similar concentrations of all five StAR proteins to preparative ultracentrifugation for 1 h at 100000*g* in both 10 mM Tris-HCl and 10 mM Tris-HCl/50 mM GnHCl. As monitored by UV adsorption at 280 nm, only 4% of the wild-type protein was precipitated by the addition of GnHCl, but substantial portions of all four mutants precipitated: E169G, 37.5%; R182L, 35.6%; ΔR272, 19.0%; L275P, 39.5%. Thus all four mutants are misfolded in a fashion that predisposes them to aggregation in low concentrations of a chaotropic agent.

DISCUSSION

StAR probably plays a role in opening a channel for the entry of cholesterol by interacting with a protein on the outer mitochondrial membrane, possibly the peripheral benzodiazepine receptor component of the mitochondrial benzodiazepine receptor complex. Bacterial expression of the active N-62 form of wild-type StAR and four of its naturally occurring amino acid replacement mutants provided milligram quantities of highly purified proteins suitable for physical characterization. The E169G, R182L, and ΔR272 mutants all reduced StAR activity to a level indistinguishable from vector control, while the L275P mutant retained 24 ± 5% of wild-type activity (*3*). These mutants were chosen because they are widely dispersed in the linear amino acid sequence and because one retained some activity and hence, presumably, some important structural features. All proteins were purified under denaturing conditions, and thus required refolding; however, native StAR had the same CD spectrum as the refolded material, indicating that the refolding protocol was successful. Analytical ultracentrifugation confirmed that all five StAR proteins were monomeric and globular.

If StAR does function as a ligand for a receptor, there are a number of ways in which point mutations could substantially impair or completely destroy its activity to promote cholesterol flow into mitochondria. First, mutation of residues that directly interact with the receptor could alter binding affinity and interfere with receptor function. Such a change might ablate StAR activity without affecting StAR's tertiary structure. Alternatively, a point mutation might affect the secondary structure of one element in the binding site and impair activity without a dramatic change in the tertiary structure. This might have a subtle effect on CD or FTIR spectra that could be difficult to characterize. A potential example of such a mutation is the introduction of a proline, which is incompatible with α-helix. Thus the L275P mutation could disrupt an α-helix, or a strategically placed proline might induce formation of a β-turn. Finally, it is possible to mutate a residue that is critical to the overall stability of protein folding, even though the secondary structure might be unaffected. Likely contributors to such a change are residues that stabilize the interactions between the various secondary structural elements. As StAR contains no disulfides, cysteine is not a candidate for such a change. However, StAR does have a large number of charged residues so that its tertiary structure is probably stabilized by salt bridges. Removal of critical charged residues could lead to misfolding, which in turn might destroy the three-dimensional structure of the binding site. Such a change would probably be evident from the melting/denaturation behavior; the E169G, R182L, and ΔR272 mutations are prime candidates for such effects.

A combination of FTIR and far- and near-UV CD spectroscopy confirmed that the wild-type and mutant StAR proteins were all folded with a substantial degree of α-helical secondary structure. However, the mutants differed significantly from the wild-type, particularly in their tertiary structure. Our data show that each of the mutations studied had some effect on StAR's structure. The L275P mutation had the least effect, consistent with its retention of some activity, and in particular it did not alter the tertiary structure in as dramatic a fashion as the charged-residue mutations. Nevertheless, L275P was more sensitive than wild-type to both urea and guanidine, indicating that its tertiary structure was weakened. By contrast, the destabilizing effects were strongest when a mutation removed an acidic or basic residue that could contribute to the electrostatic stabilization of the tertiary structure. Unlike the L275P mutant, each of the charged-residue mutants displayed strong intermolecular β-sheet structures when dried as a thin film, suggesting that surfaces normally buried in the wild-type became exposed in the misfolded mutants. The unusually low frequency of the signal for the intermolecular β-sheet might be explained by an additional contribution from electrostatic forces.

We propose that the diminished or absent activity of the StAR mutants is primarily due to protein misfolding. Mutations of charged residues apparently disrupted salt bridges, exposing surfaces that are normally buried. These mutants tend to associate on drying and in the presence of low concentrations of GnHCl. In addition to altering the over-all conformation of the StAR protein, we propose that the misfolding specifically disrupts the binding site for a StAR receptor on the outer mitochondrial membrane, thus

preventing the receptor−ligand interaction, and causing lipoid CAH.

ACKNOWLEDGMENT

We thank Dr. David A. Agard, Department of Biochemistry and Biophysics, for the use of the CD spectropolarimeter, Dr. Stanley B. Prusiner, Department of Neurology, for the use of the FTIR spectrophotometer, and Drs. Eric D. Anderson and Claus Agard for assistance with the analytical ultracentrifugation and for productive discussions. H.B. thanks the other members of the Miller laboratory for their advice and cooperation.

REFERENCES

1. Miller, W. L. (1988) *Endocr. Rev. 9*, 295−318.
2. Clark, B. J., and Stocco, D. M. (1996) *Endocr. Rev. 27*, 221−244.
3. Lin, D., Sugawara, T., Strauss, J. F., III, Clark, B. J., Stocco, D. M., Saenger, P., Rogol, A., and Miller, W. L. (1995) *Science 267*, 1828−1831.
4. Sugawara, T., Holt, J. A., Driscoll, D., Strauss, J. F., III, Lin, D., Miller, W. L., Patterson, D., Clancy, K. P., Hart, I. M., Clark, B. J., and Stocco, D. M. (1995) *Proc. Natl. Acad. Sci. U.S.A. 92*, 4778−4782.
5. Bose, H. S., Sugawara, T., Strauss, J. F., III, and Miller, W. L. (1996) *N. Engl. J. Med. 335*, 1870−1878.
6. Hum, D. W., and Miller, W. L. (1993) *Clin. Chem. 39*, 333−340.
7. Epstein, L. F., and Orme-Johnson, N. R. (1991) *J. Biol. Chem. 266*, 19739−19745.
8. Stocco, D. M., and Sodeman, T. C. (1991) *J. Biol. Chem. 266*, 19731−19738.
9. Clark, B. J., Wells, J., King, S. R., and Stocco, D. M. (1994) *J. Biol. Chem. 269*, 28314−28322.
10. Tee, M. K., Lin, D., Sugawara, T., Holt, J. A., Guiguen, Y., Buckingham, B., Strauss, J. F., III, and Miller, W. L. (1995) *Hum. Mol. Genet. 4*, 2299−2305.
11. Nakae, J., Tajima, T., Sugawara, T., Arakane, F., Hanaki, K., Hotsubo, T., Igarashi, N., Igarashi, Y., Ishii, T., Koda, N., Kondo, T., Kohno, H., Nakagawa, Y., Tachibana, K., Takeshima, Y., Tsubouchi, K., Strauss, J. F., III, and Fujieda, K. (1997) *Hum. Mol. Genet. 6*, 571−576.
12. Hauffa, B. P., Miller, W. L., Grumbach, M. M., Conte, F. A., and Kaplan, S. L. (1985) *Clin. Endocrinol. 23*, 481−493.
13. Saenger, P., Klonari, Z., Black, S. M., Compagnone, N., Mellon, S. H., Fleischer, A., Abrams, C. A. L., Shackleton, C. H. L., and Miller, W. L. (1995) *J. Clin. Endocrinol. Metab. 80*, 200−205.
14. Miller, W. (1997) *J. Mol. Endocrinol. 17*, 227−240.
15. Sugawara, T., Lin, D., Holt, J. A., Martin, K. O., Javitt, N. B., Miller, W. L., and Strauss, J. F., III (1995) *Biochemistry 34*, 12506−12512.
16. Arakane, F., Sugawara, T., Nishino, H., Liu, Z., Holt, J. A., Pain, D., Stocco, D. M., Miller, W. L., and Strauss, J. F., III (1996) *Proc. Natl. Acad. Sci. U.S.A. 93*, 13731−13736.
17. Papadopoulos, V. (1993) *Endocr. Rev. 14*, 222−240.
18. Bose, H. S., Pescovitz, O. H., and Miller, W. L. (1997) *J. Clin. Endocrinol. Metab. 82*, 1511−1515.
19. Sambrook, J., Fritsch, E. F., and Maniatis, T. (1989) in *Molecular Cloning: A Laboratory Manual*, pp 17.32 and A2, Cold Spring Harbor Laboratory Press, Plainview, NY.
20. Gill, S. C., and von Hippel, P. H. (1989) *Anal. Biochem. 182*, 319−326.
21. Greenfield, N. J. (1996) *Anal. Biochem. 235*, 1−10.
22. Rost B., and Sander, C. (1993) *Proc. Natl. Acad. Sci. U.S.A. 90*, 7558−7562.
23. Yang, J. T., Wu, C.-S., and Martinez, H. M. (1986) *Methods Enzymol. 130*, 208−269.
24. Manavalan, P., and Johnson, W. C., Jr. (1987) *Anal. Biochem. 167*, 76−85.
25. Sreerama, N., and Woody, R. W. (1993) *Anal. Biochem. 209*, 32−44.
26. Matthews, C. R. (1993) *Ann. Rev. Biochem. 62*, 653−683.
27. Creighton, T. E. (1993) in *Proteins*, pp 71−260, W. H. Freeman and Co., New York.
28. Ptitsyn, O. B., and Semisotnov G. V. (1991) in *Conformations and Forces in Protein Folding* (Nall, B. T., and Dill, K. A., Eds.) pp 155−168, American Association for the Advancement of Science, Washington, DC.
29. Woody, R. W., and Dunker, A. K. (1996) in *Circular Dichroism and Conformational Analysis of Biomolecules* (Fasman, G. D., Ed.) pp 109−144, Plenum Press, New York.
30. Mant, C. T., Zhou, N. E., and Hodges, R. S. (1993) in *The Amphipathic Helix* (Epand, R. M., Ed.) pp 39−64, CRC Press, Boca Raton, FL.
31. Goormaghtigh, E., Cabiaux, V., and Ruysschaert, J.-M. (1993) in *The Amphipathic Helix* (Epand, R. M., Ed.) pp 67−86, CRC Press, Boca Raton, FL.
32. Krimm, S., and Bandekar, J. (1986) in *Advances in Protein Chemistry* (Anfinsen, C. B., Edsall, J. T., and Richards, F.M., Eds.) pp 181−364, Academic Press, Orlando, FL.
33. Byler, D. M., and Susi, H. (1986) *Biopolymers 25*, 469−487.
34. Surewicz ,W. K., and Mantsch, H. M. (1988) *Biochim. Biophys. Acta 952*, 115−130.
35. Goormaghtigh, E., Cabiaux, V., and Ruysschaert, J.-M. (1990) *Eur. J. Biochem. 193*, 409−420.
36. Tanford, C. (1970) *Adv. Protein. Chem. 24*, 1−99.
37. Pace, C. N. (1986) *Methods Enzymol. 131*, 266−280.

BI980588A